An investigation on the relationships between the petrographic, physical and mechanical characteristics of sandstones from Newspaper Member of the Natal Group using Self Organising Maps

Ferentinou Maria[1*]

[1] University of Johannesburg, Johannesburg, South Africa

Sandstone is the most significant rock type in the Natal Group, and widely extended into the Marianhill Formation. Due to prevalence within the Natal Basin it is widely used as aggregate material therefore it is important to study the physical properties and their relative effect to the mechanical properties. Literature is rather limited, so this study is attempting to investigate the published data, applying the approach of self-organising maps and data-mining techniques in order to extract new knowledge and give further insight into the relationships amongst sandstone petrographic, physical and mechanical characteristics. SOM-based analysis distinguished three clusters, with similar petrographic, physical, geotechnical characteristics, which led to the identification of different lithofacies. Significant parameters dictating cluster identification, are the type of grain contact, void space, packing density, and amount of silica cement.

INTRODUCTION

The sandstones studied in the current paper fall under the Natal Group which is a succession of reddish grey sandstones with subordinate silt-stones, shales and conglomerates, regarded as molasses deposit accumulated 490Ma ago, Thomas et al. (1992). The great majority of the sediments of the Natal Group were deposited in a fluvial environment and represent a terrestrial succession, interrupted by occasional shallow marine transgressions during which quartz arenites were deposited, Marshall (1994). Thickness of the Group ranges from 45 to 600m, of which Newspaper member comprises some 80%. Marshal (1994), recognised two formations within the Natal Group, the lower Durban Formation, and the upper Marianhill Formation, which is subdivided into three members, from the oldest to the youngest Tullini, Newspaper, and Westville member. The Newspaper member comprises 90% of the Marianhill Formation, and occurs over the whole of the Natal Group basin. The most important sedimentary feature is the planar cross bedding.

The data set published by Bell & Lyndsay (1999) came from a borehole at Kloof, close to Durban. The core was sampled at approximately 10m intervals to a depth of 300m, with the aim of determining the extent to which the petrographic properties influence the mechanical properties of this lithology.

Many studies (Bell, 1978, Dobereiner and De Freitas, 1986, Ulusay et al., 1994) confirm that the geomechanical properties of a sandstone vary widely, which has generally attributed to the petrographic characteristics. Some of these properties include grain size distribution, packing density, packing proximity, type of grain contact, length of grain contact, amount of void space, type and amount of cement/matrix material and mineral composition.

The usual methods for studying petrographical, physical and geomechanical properties include:

(i) comparison of the values range and their general trend;

(ii) statistical analysis, mainly by means of correlation coefficients and linear regression analyses, searching for interrelationships between the various measured parameters.

In this paper the application of Artificial Neural Networks (ANN) is proposed in order to investigate lithofacies identification. ANN are data processing techniques useful for modelling large amounts of data, particularly when the relationships between the various factors are non-linear, and not immediately apparent. ANN, which make use of non-linear transformation functions have complex structures themselves, and can be employed to interpret complex geomorphologic processes such as sedimentary systems.

A widely applied method in data mining, used as a clustering tool is Self Organising Maps (SOM), which is a clustering and projection algorithm of high-dimensional data to a lower dimensional space (Kohonen, 1995). SOM is a special type of Artificial Neural Network (ANN) that is trained using unsupervised learning to produce a low-dimensional projection of the input space, called the map. SOM, has been used previously for successfully clustering items in various geo-environmental studies (Ferentinou & Sakellariou 2005, 2007; Ersoya et al. 2007; Tselentis et al. 2007; Ferentinou et al. 2012, Karymbalis et al. 2016, Park et al., 2016). Unsupervised neural networks, which were used in this study, are trained by letting the network continually adjust itself to new inputs. They can uncover non-linear relationships within data, define classification schemes that adapt to changes in new data, and reveal new patterns. Among the advantages of ANNs is that they conserve the complexity of the systems they model (here, the sedimentation of the Newspaper member). They also encode information about their environment in a distributed form and have the capacity to self-organize their internal structure. The principal results from this study refer to the identification of clusters in the original multivariate data set. SOM-based analysis distinguished three clusters, with similar petrographic, physical, geotechnical characteristics, which led to the identification of different lithofacies. Trends that are not clearly detected in the whole data set, were clearly identified at cluster level.

DATA AND MATERIALS

Mineral Composition

Bell and Lindsay, (1999) found in a scanning electron microscope study that the Newspaper Member is composed mainly of quartz, ranging from 52.3 to 83.6% and the total feldspar content ranges from 7 to 31%. They also examined the surface texture of quartz grains, and found that there were distinctive surface features on quartz grains, which indicated erosion and transportation, or deposition by subsequent diagenetic processes. Evidence of dissolution of quartz, and cleavage surfaces were identified. The amount and type of cement was found to be very variable. Cement types include silica up to 12%, calcite up to 10%. Clay minerals content was found to be up to 23%, including authigenic chlorite. These occupied most of the void space at times. The mineral composition of the Newspaper member sandstones appears, in Table 1. According to the classification scheme of Folk (1974), the majority of these sandstones are arkosic arenites with secondary subarcosic arenites.

.

Grain properties

Most of the grains were subangular, ranging between 38 and 51%, whereas subrounded grains were ranging between 26 to 44%, then followed angular, very angular and rounded followed in that order. Bell and Lindsay, (1999), also investigated the type of contact as it is a measure of the stress to which the grains have been subjected. The majority of grain contacts were found to be concavo-convex and long-types, average values being 26.5 and 28.5% which according to Taylor (1950) and the same authors is an indication that these sandstones have undergone a significant amount of high overburden pressure. Few contacts were found to be tangent and sutured, average values 7.3 and 6.3 % respectively.

In many samples, it was noticed that the grain to cement contact is the most common type of contact.

The arrangement of particles in a sandstone packing, is defined as the mutual spatial relationship among grains Kahn, (1956), suggested that packing can be assessed through packing proximity and

packing density. Packing proximity ranged from 37 to 77%, and packing density from 66 to 96%.

Density, porosity and permeability

The range of specific gravity of the samples showed little variation ranging from 2.66 to 2.70. Dry density showed also little variation extending from 2.40 to 2.54 mgm^{-3}. The effective porosity was measured with an air porosimeter and varied from 3.4 to 9.3%. The permeability of these sandstones was measured using an Ohle permeameter, using nitrogen as the permeating fluid. The permeability values varied from 2.89^{-13} to 5.87^{-9} ms^{-1} which indicates that they are essentially impermeable, hence permeability was not included in the current study.

Strength, hardness and deformability

The range of unconfined compressive strength varied between 77 and 214MPa. The sandstones underwent remarkable reduction in unconfined compressive strengths when compared with their dry equivalent. The Brazilian strength of these sandstones varied from 6 to 20MPa, and the diametral point load strength fell within the range of 4 to 13MPa, with an average ratio of unconfined to compressive strength to the diametral point load strength (MR) of 14.7.
The hardness of these sandstones was determined by the Shore scleroscope and the Schmidt hammer. The range of values for Shore hardness extended from 50 to 96, and for Schmidt hammer, varied between 39 and 49.
Elastic properties determined were Young's modulus (Et_{50}), and Poisson's ratio (v). The average value of Young's modulus was 50.8GPa. The range of Poisson's ratio had a mean value of 0.255. The modulus ratio (Et_{50}/unconfined strength), has a mean value of 372.

METHODOLOGY

To investigate the clustering tendency of the petrographic, physical and mechanical characteristics of variables describing sandstone petrographic, physical and geomechanical characteristics, SOM was applied. SOM is an unsupervised ANN formed from 'neurons' located on a regular array grid, which is usually two-dimensional. SOM is capable of mapping high-dimensional similar input data into clusters according to similarities in the variables. All the calculations in this study were performed using Matlab v.12b software applying SOM Toolbox 2.0 (Vesanto, 1999). A general architecture of SOM consists of input nodes (map units), output nodes and weight parameters. Each input node is fully connected to the output nodes through variable connections. SOM eventually settles into a map of stable zones – the clusters. Each zone is effectively a feature classifier, so the graphical output of this kind of analysis can be characterized as a type of feature map of the input space (n-dimensional input data) projected on to a lower dimensional output grid. Any new, previously unseen input vectors presented to the network stimulate nodes in the zone (cluster) with similar weight vectors. Each unit i is represented by a prototype vector $m_i = [m_{i1}, ..., m_{in}]$ where n is input vector dimension. The units are connected to adjacent map units by a neighbourhood function. The number of map units determines the accuracy and generalization capacity of SOM. During the training process, the SOM algorithm forms an elastic net that folds onto the cloud formed by the input data. Data points lying near each other in the input space are mapped onto nearby map units in the map (Kohonen, 1995). In each training step, a multivariate input vector x from the input dataset is chosen randomly and the distance between x and all the weight vectors (m_i) of the SOM is calculated by using an Euclidean measure of distance. The neuron with the weight vector that is closest to x, is called the best-matching unit (BMU), signified by the subscript c. The input is simply mapped in this location:

$$\| x - m_c \| = \min\{\| x_t - m_t \|\} \quad [1]$$

where $\| \cdot \|$ is the linear distance between x and m_c typically Euclidean distance. After finding the BMU, the weight vectors of the SOM are updated so that the BMU is moved closer to the input vector in the input space: the new vector x. The topological neighbours of the BMU are treated similarly. During learning, or the process of nonlinear projection, those nodes that are topologically close in the array up to a certain geometric distance will activate each other to learn something from the learning input x. The updated rule for the weight vector *i* is:

$$x_i(t+1) = m_i(t) + a(t)h_{ci}(t)[x(t) - m_i(t) \quad [2]$$

where $x(t)$ is an input vector that is randomly drawn from the input data set, $a(t)$ is the learning rate and t denotes time. A Gaussian function $h_{ci}(t)$ is the neighbourhood kernel around the winning unit m_c and a decreasing function of the distance between nodes i and c on the map grid. This non-linear regression is usually reiterated over all the available input vectors. This process is usually reiterated over the available samples with decreasing neighbourhood and update functions (i.e. learning rate), which in continued learning leads to a global ordering. There are a number of training parameters that need to be decided before training to attain convergence. These parameters are the number and shape of the SOM map units, the neighbourhood kernel function, the neighbourhood radius, the learning rate and epochs training. The map size was 10 × 10 and the neighbourhood kernel function was Gaussian. The shape of the map units (circle, hexagonal or square) is important, not only for visualization purposes, but for the training as well, as it is related to the neighbourhood function. The training parameters are generally defined through a trial and error process, or the user can rely on the default suggested values. Two evaluation criteria are typically used to measure the quality of training: resolution and topology preservation. The measures of the quality of the map are:

(i) q_e the average distance between each data vector and its BMU, which measures map resolution;

(ii) t_e the topographic error, which is the proportion of all data vectors for which the first and the second BMUs are not adjacent units – this is a measure of topology preservation (Kohonen, 1995).

SOM was trained with different numbers of map units and the optimum map size and normalization method was selected according to the minimum quantization error (q_e) and topographic error (t_e). In this study, q_e was 0.31 and t_e was 0.001, were obtained using logistic normalization, which scales all possible values between [0,1]. Learning rate was set to 0.5, neighbourhood radius was initially set to 3 and then during finetuning was set to 1. The SOM network was trained in two phases: a rough training with a large initial neighbourhood radius width and a fine-tuning phase with a small initial neighbourhood radius. The SOM algorithm was applied as an efficient classification and visualization tool for an n-dimensional data set. To interpret the results, the SOM Toolbox was implemented to benefit from its efficient visualization techniques. One problem with the visualization of multidimensional information is that the number of properties that need to be visualized is higher than the number of available visual dimensions. The SOM Toolbox (Vesanto, 1999; Vesanto & Alhoniemi 2000) offers a solution to use many visualizations linked together so that the same object can immediately be identified from the different visualizations. When several visualizations are linked together, scanning through them is very efficient because they are interpreted in a similar way.

RESULTS

The characteristics that were investigated are, Quartz, K-feldspar, Plagioclase, lithics, mica, opaques, amount of calcite cement, amount of silica cement, and amount of clay content. Type of contact was also described, namely (tangent, long types, concavo-convex), sutured (expression of contact type as one numerical value), and number of floating or non-contacts expressed in terms of grain to cement to matrix and to void, (cement/matrix void,). Packing proximity and packing density, density, porosity and effective porosity, strength hardness and deformability were also described and analysed.

The results of the SOM analysis are presented through various visualizations of the self organized map in (Figs. 1, 2 and 3). Fig. 1 consists of 33 rectangular maps with hexagonal map units. The first map on the upper left is a U-matrix, with colours indicating similarity between adjacent nodes through colour coding (cooler colours indicate proximity whereas hotter indicate distance). The 31 component layer plots, one for each input variable, follow in Figure 1.
Relationships between various properties that characterize general trends in the data set (independently of the following clustering) can be seen through visual inspection of the respective component layer plots in Figure 1. For example, concavo-type of contact convex and total weighted contact value are well correlated, since they present the same colour code for both component planes, for the majority of the hexagonal map units across the component layer, (position color similarity).
Total weighted contact value is a significant value for cluster 2. Shows inverse correlation with cement content and amount of clay minerals. Packing density and packing proximity is well correlated to the total type weighted contact value. Packing density is inversely correlated to the cement content for cluster 2, but shows positive correlation for clusters 1 and 3. Packing density and packing proximity have a significant relationship in cluster 2. Packing proximity had an inverse correlation with clay content especially for cluster 1 and 2, and cement amount for cluster 3. Density and effective porosity are well correlated, though porosity varies throughout the three clusters.
General trends between clay content, and quartz content were not identified, but further correlations could be detected at cluster level. Quartz content and K-feldspar are inversely correlated. Density, effective porosity, Point Load Index, Schmidt hammer hardness number, Young modulus and Poisson ratio are well correlated. UCS, Brazilian strength, shore hardness, is another group of training parameters which are well – correlated.
Types of hardness were not influenced by the petrographic parameters, hardness is correlated to density.
Schmidt hardness is strongly correlated to Point Load Index strength index, but not to Brazilian strength.
Quartz content, cement content and amount of clay minerals did not seem to accrue significant within the data set.
Dry density and Young's modulus presented high correlation. Effective porosity, with Young's modulus and Poisson ratio showed high correlation as a general trend.
Yet there were no significant correlation noticed between absolute and effective porosity.
The expected negative correlation between effective porosity could be due to the impermeable character of the sandstone.

Classification of sandstone samples

SOM segmented the data set into three individual clusters according to the number of samples that constitute the particular cluster at the particular depth. Using the k-means algorithm, Principal Component analysis and Davies–Bouldin Index (DBI, Davies and Bouldin, 1979) (Fig. 3), three clusters were recognized. The color coding followed is magenta for cluster 1, green for cluster 2, deep purple for cluster 3. The response of the given data to the map (signal hits–BMUs number) (Fig. 2) for each cluster was summed as a cluster index value. The higher the cluster index value the stronger the cluster and therefore the most important in the data set. The observed characteristics were ordered from the most to the least frequent in the cluster. The properties whose visual representation through component layer resembles most the boundaries of the cluster were identified and they were acknowledged as the most important parameters.

Cluster 1: Eight samples, were classified in this cluster. The characteristics of the cluster are high number of floating or non-contacts to void, high Quartz %, low K-feldspar % and Lithics, low Mica, low amount of calcite cement, low amount of silica cement, low clay minerals content. High porosity, low density and effective porosity. Low UCS value, low Brazilian Strength value, high Modulus ratio value. The index for this cluster is 8. The most important parameters for this cluster are Quartz %, Lithics, cement silica, porosity, and UCS value. The depth range of that lithotype is 17.3 to 117.3 m.

Cluster 2: Five samples, were classified in this cluster. The characteristics of the cluster are, most types of contacts are concavo-convex, high total weighted contact, low amount of calcite cement, low number of floating or non-contacts to void, high packing proximity, high packing density. Quartz % varies, high K-feldspar %, low Plagioclase %, low amount of cement silica, low percentage of clay minerals. Porosity, UCS, Brazilian strength and Shore hardness, and Modulus ratio vary, indicating for a further subdivision of this cluster to two sub-clusters. The index for this cluster is 5. The most important parameters are type of contact long, concavo-convex, total weighted contact, cement, packing density, K- feldspar, and amount of silica cement. The depth range for this lithotype is 142.2 to 204.8m

Cluster 3: Twelve samples were classified in this cluster. The characteristics of the cluster are prevalence of tangent type contacts, and low concavo-convex type of contacts, low total weighted contact, medium amount of silica cement, high amount of clay minerals, high number of floating or non-contacts to matrix value, high number of floating or non-contacts to void, low packing proximity, low packing density, low quartz percentage, high K-feldspar percentage, low clay minerals percentage, and low porosity. Uniaxial compressive strength values are high in this cluster, Brazilian strength values are high, Shore hardness index is high, and modulus ratio is high. The index for this cluster is 11, and appears to be the strongest in the data set. The depth range for this cluster is 206.5 to 302.1m, but similar characteristics are also noted at the depth of 84.2m.

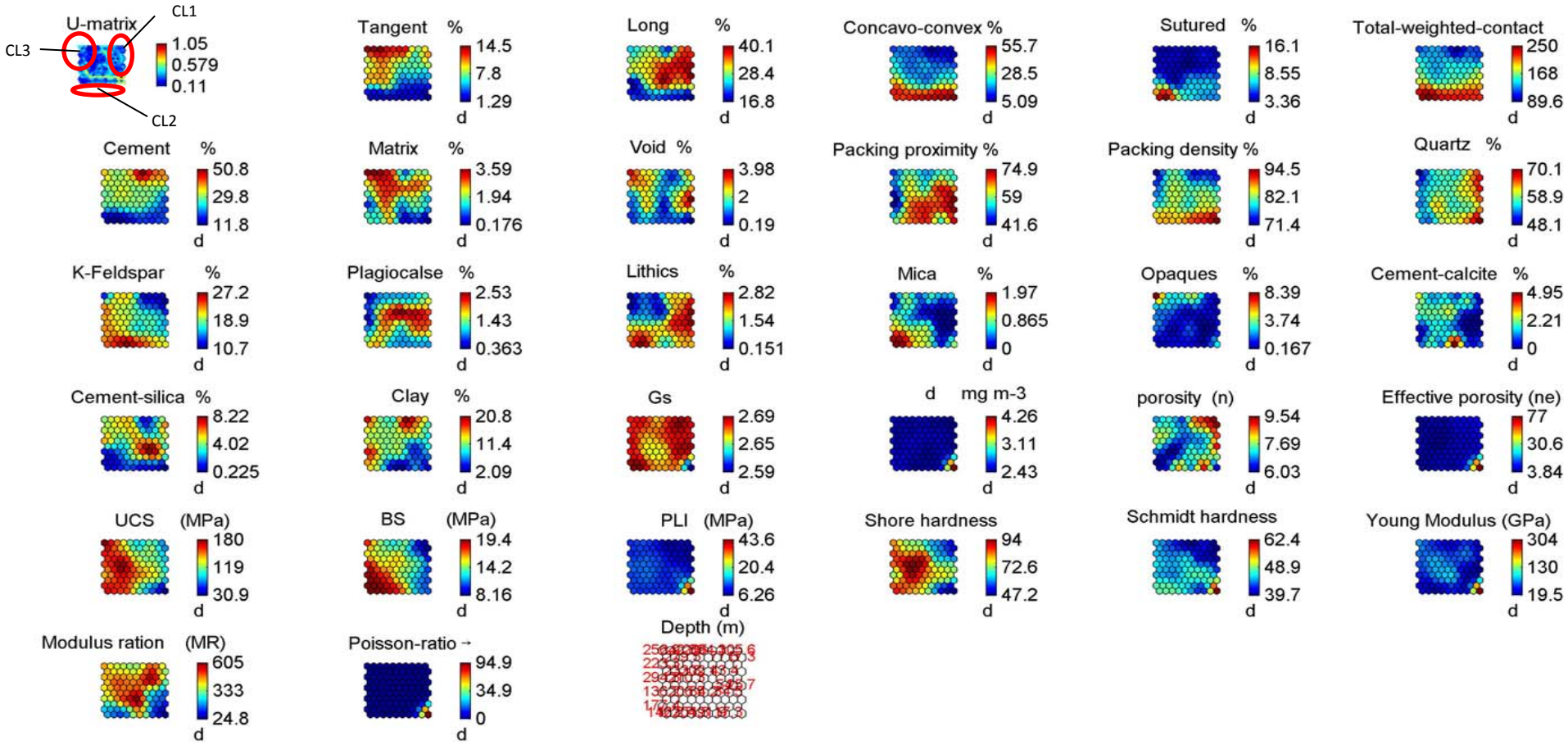

Figure 1. Clustering visualizations using similarity colouring for petrographic, physical and mechanical properties. U-matrix (top left) with cluster distribution and 31 component plane plots, one for each parameter.

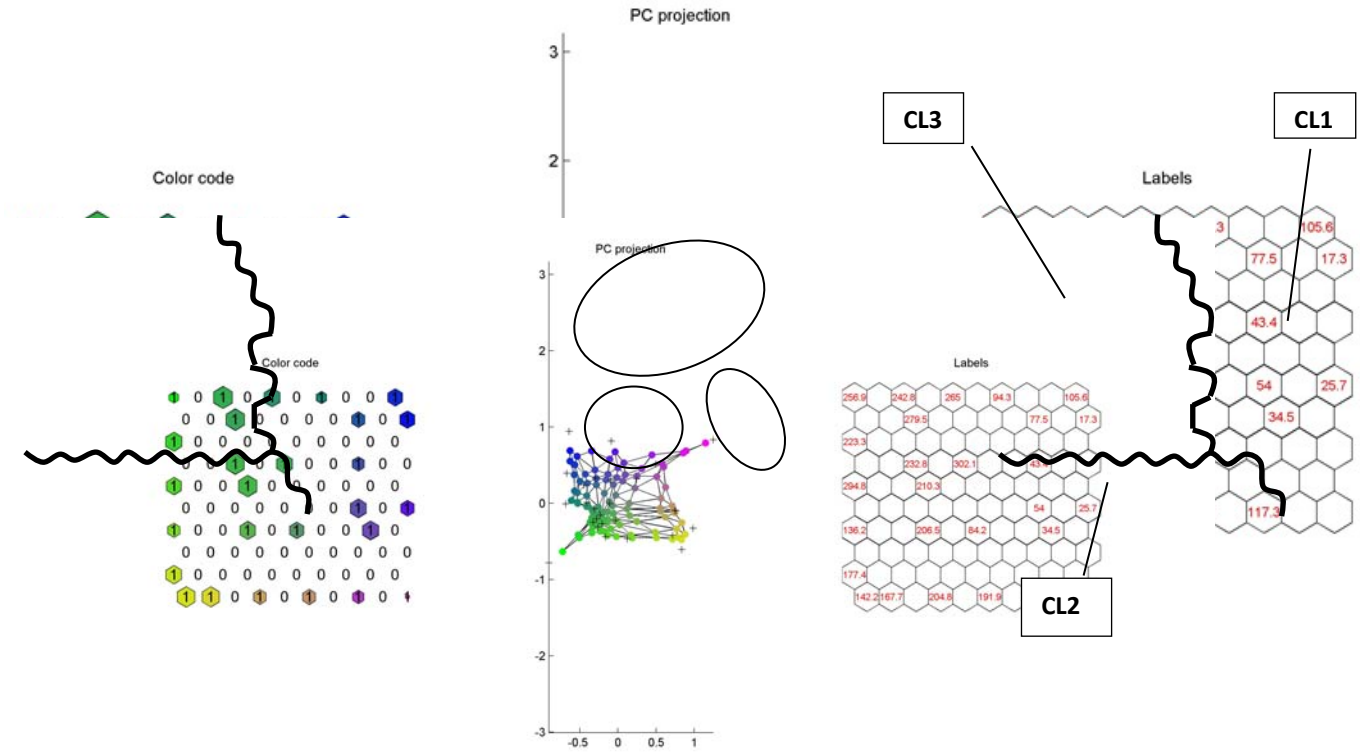

Figure 2. Clustering visualizations, using k-means algorithm, and principal component analysis.

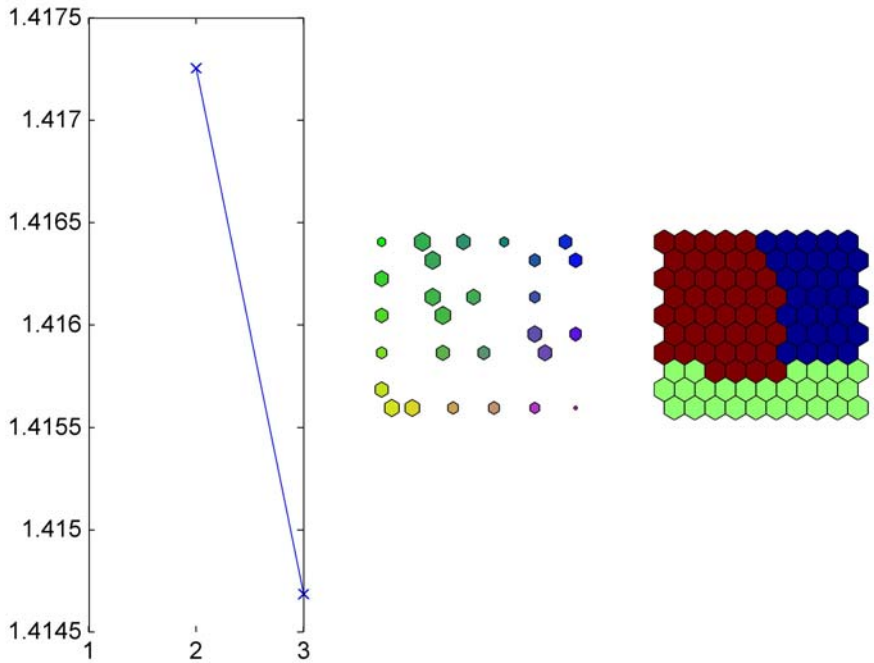

Figure 3. The Davies-Bouldin index seems to indicate that there are 3 clusters on the map.

DISCUSSION AND CONLCUSION

SOM classification shows that clustering of petrographic, physical, and geotechnical properties, is generated according to certain burial depth intervals, indicating certain lithotypes.
It is confirmed through the application of unsupervised neural networks training, (SOM), that the geomechanical properties vary widely, and that they are not only related to the petrographic characteristics but also to the packing density, packing proximity, type of grain contact, length of grain contact, amount of void space, and amount of cement / matrix.
It is important to mention that the produced smart visualisations offer the opportunity to identify correlations within the cluster, and detect cluster level correlation which could be masked at data set level.
According to Bell and Lindsay (1999), packing proximity presents a wide range, which is also confirmed through the current analysis. However, if this observation is combined with the type of contact prevailing per cluster and adequate depth levels, this could lead to the conclusion that Cluster 1 in depth less than 90m, medium to high values of packing proximity prevail, and long type of contacts. Low values of packing proximity indicate high cement %. In Cluster 2 in depths ranging from 90 to 200m, high values of packing proximity prevail and the types of contacts are concavo-convex, and cement % is very low.
Density is highly correlated to effective porosity values. Uniaxial compressive strength component layer clearly indicates three decipherable clusters, which is proposed also by Brazilian strength component layer and shore hardness.
Bell and Lindsay (1999), suggest that the various petrological properties had little or no influence on the mechanical properties or behaviour of the sampled sandstones. SOM analysis revealed that UCS values would correlate with percentage of tangential type of contacts, cement content, and matrix, amount of silica cement. Point Load strength showed correlation with packing density.
The relationships between the mechanical properties themselves proved to be more distinct, and identify a clear general trend. It should be noted though that the mechanical properties data set is based on measurement and empirically based indices, and tools, that have an inherent lower epistemic uncertainty. Whereas all the parameters related to petrographic and mineralogical properties tend to include an inherent higher epistemic uncertainty, due to the fact that they are sedimentation process related. A larger more representative data set would allow for further generalisations and conclusion.

Table I. Petrographic, physical and geomechanical properties of the Newspaper Member

Type of Contact and packing										Mineral composition								Density and porosity				Geomechanical properties								
Tangent %	Long %	Concavo-convex %	Sutured %	Total weighted contact	Cement %	Matrix %	Void %	Packing_proximity %	Packing_density %	Quartz %	K- Feldspar %	Plagioclase %	Lithics %	Mica %	Opaques %	Cement-calcite %	Cement-silica %	Clay %	Specific gravity	Dry density mg m^{-3}	Absolute porosity %	Effective porosity %	UCS (Mpa)	BS (Mpa)	PLI axial value (Mpa)	Shore hardness	Schmidt hardness	Young's modulus (GPa)	Modulus ratio	Poisson ratio	Depth of sample (m)
12	37	7	4	123	35	3	2	56	76	72	8	2	4			0	10	4	2.68	2.43	9.3	8.9	84	6	6	49	39	19.5	232	0.36	17.3
6	44	21	5	177	18	1	5	77	81	68	15	2	3		1	0	2	11	2.69	2.42	10	8.8	88	10	7	71	41	14.3	163	0.28	25.7
2	32	35	8	203	18	2	3	77	84	54	16	2	2			0	8	6	2.69	2.49	7.5	6.7	136	11	13	80	49	26.8	197	0.22	34.5
8	39	18	3	152	27	3	2	77	82	61	17	3	2		1	0	2	14	2.68	2.5	6.8	6.5	107	14	7	64	38	72.6	679	0.14	43.4
7	34	15	5	140	35	2	2	61	83	62	20	2	3			0	12	2	2.69	2.51	6.7	6.2	141	15	11	76	48	28.2	200	0.14	54
4	38	12	6	140	37	3	0	60	77	61	13	1	2		1	4	2	15	2.7	2.47	8.5	7.7	141	9	9	64	44	85.6	607	0.2	77.5
4	43	15	7	163	30	1	0	70	79	56	16	1	2	1	2	1	6	13	2.66	2.42	7.7	6.8	147	14	10	81	48	99.9	680	0.41	84.2
15	14	1	3	58	66	0	1	51	72	55	10	1	2	1	5	0	0	27	2.68	2.46	9	8.7	93	15	5	63	39	33.2	357	0.21	94.3
9	34	10	3	119	40	1	4	56	74	62	13	1	1	1	1	0	2	19	2.69	2.42	10.1	9.3	80	10	8	57	40	35.4	443	0.3	106
3	20	51	6	220	18	1	1	52	89	63	22	1	2			0	1	9	2.68	2.4	10	9.1	77	12	9	50	40	10.9	141	0.18	117
12	13	35	7	171	32	0	1	37	79	52	23	1	2	1	2	0	0	21	2.68	2.5	6.7	5.6	133	19	11	68	44	53.1	399	0.29	136
2	26	40	21	258	9	2	0	58	86	52	25	2	2	2		0	1	14	2.69	2.52	6.3	4.4	184	20	11	96	47	56.6	307	0.36	142
2	18	44	22	258	11	1	2	69	86	52	24	2	4	2	1	4	1	12	2.7	2.53	6.4	6	148	19	11	80	49	15.2	103	0.19	168
2	16	53	8	225	18	2	1	50	85	60	20	1	2	2	1	0	1	15	2.69	2.54	5.6	4.5	157	19	12	82	49	30	191	0.33	177
1	16	57	6	216	20	0	0	75	96	72	20	1	2		1	3	1	0	2.68	2.51	6	5.8	141	16	11	75	46	78.8	558	0.29	184
2	20	51	7	223	19	0	1	72	89	60	24	1	1	1	1	10	1	0	2.67	2.5	6.4	5.6	112	17	11	74	45	55.5	495	0.33	192

Tangent %	Long %	Concavo-convex %	Sutured %	Total weighted contact	Cement %	Matrix %	Void %	Packing_proximity %	Packing_density %	Quartz %	K- Feldspar %	Plagioclase %	Lithics %	Mica %	Opaques %	Cement-calcite %	Cement-silica %	Clay %	Specific gravity	Dry density mg m^{-3}	Absolute porosity %	Effective porosity %	UCS (Mpa)	Brazilian strength (Mpa)	Point Load axial value (MPa)	Shore hardness	Schmidt hardness	Young's modulus (GPa)	Modulus ratio	Poisson ratio	Depth of sample (m)
2	23	50	8	230	13	3	1	67	85	61	29	1	2	1	1	0	2	3	2.67	2.43	9	6.9	160	19	11	80	48	24.7	154	0.35	205
11	30	24	3	155	28	3	3	68	83	64	20	2	2	1		2	2	11	2.66	2.51	5.6	5.4	161	18	13	94	44	82.3	511	0.23	207
10	32	14	4	132	35	3	2	65	84	59	22	2	1		1	1	3	11	2.66	2.57	5.6	2.4	214	15	13	98	45	83.5	386	0.44	210
7	28	24	4	155	32	2	3	53	76	53	26	1			1	2	4	12	2.68	2.47	7.8	5.7	158	14	10	85	45	65.7	416	0.18	223
11	30	18	4	141	31	3	3	61	83	57	18	2	1	1	2	3	4	12	2.67	2.44	8.6	4.4	163	15	12	92	45	94.6	580	0.31	233
18	26	21	3	145	26	4	2	54	81	58	22	1	1	1	2	1	5	10	2.69	2.48	7.8	6.1	156	14	13	74	44	52.2	335	0.29	243
16	24	11	4	113	37	4	4	46	66	43	7				20	3	4	23	2.68	2.5	6.7	3.4	192	19	11	82	46	86.2	450	0.45	257
12	29	15	4	131	35	3	2	52	80	59	22	1			3	2	6	8	2.66	2.5	6	4.5	102	12	10	73	40	32.1	314	0.36	265
11	32	14	5	137	32	3	3	66	83	56	20	1	1	1	3	1	5	12	2.68	2.49	7.1	6.8	134	14	10	70	43	54.8	408	0.21	280
9	33	24	4	163	27	2	1	40	77	56	21		1	1	2	2	7	11	2.69	2.47	8.1	6.4	157	19	13	86	47	61	388	0.15	295
7	36	22	3	157	28	3	1	53	81	58	18	3				3	6	12	2.68	2.5	6.7	6.2	123	16	11	91	47	58.4	445	0.34	302

REFERENCES

Bell, F.G. (1978). The physical and mechanical properties of the Fell Sandstones, Northumberland, England. Engineering probably Geology (12), 1–29.

Bell, B.G. and Lindsay, P. (1999). The petrographic and geomechanical properties of some sandstones from the Newspaper Member of the Natal Group near Durban, South Africa, Engineering Geology, (53), Issue 1, 57-81.

Davies, D.L. and Bouldin, D.W. (1979). A cluster separation measure. IEEE Transactions on Pattern Analysis and Machine Intelligence PAMI-1 (2), 224–227.

Dobereiner, L. and De Freitas, M.H. (1986). Geotechnical properties of weak sandstone. Geotechnique (36), 79–94.

Ersoy, O., Aydar, E., Gourgaud, A., Artuner, H. and Bayhan, H. (2007). Clustering of volcanic ash arising from different fragmentation mechanisms using Kohonen self-organizing maps. Computers & Geosciences, 33(6), 821-828.

Ferentinou, M., Hassiotis T, and Sakellariou M. (2012). Application of computational intelligence tools for the analysis of marine geotechnical properties in the head of Zakynthos Canyon, Greece, Computers and Geosciences, (40), 166-174.

Ferentinou M. and Sakellariou M., (2015). Introduction of an objective matrix coding method for rock engineering systems through self – organizing maps. The 13th International congress of rock Mechanics, ISRM congress 2015, Canada, ISBN: 978-1-926872-25-4

Folk, R.L. 1974. Petrology of Sedimentary Rocks. Hemphill, Austin.

Karymbalis, E., Ferentinou, M., and Giles, P. (2016). Using morphometric variables and self-organising maps to identify clusters of alluvial fans and catchments in North Peloponnese, Greece, in Geology and Geomorphology of Alluvial and Fluvial Fans: From Terrestrial to Planetary Perspectives, GSL Special Publications, (440), 10(3): 455–478.

Kahn, J.S., 1956. The analysis and distribution of the properties of packing in sand size sediments. 1. On the measurement of packing in sandstones. Journal of Geology (64), 385–395.

Kohonen, T. (1994). Self - Organising Maps. Springer.

Park, J., Yang, G., Satija, A., Scheidt, C. and Caers, J. (2016). DGSA: A Matlab toolbox for distance-based generalized sensitivity analysis of geoscientific computer experiments. Computers and Geosciences, (97), 15-29.

Marshall, C.G.A. (1994). The stratigraphy of the Natal Group. Unpublished M.Sc. thesis, University of Natal, Pietermaritzburg.

Taylor, J.M., (1950). Pore space reduction in sandstone. Bulletin American Association of Petroleum Geologists (34),701–716.

Tselentis, G.A., Serpetsidaki, A., Martakis, N., Sokos, E., Paraskevopoulos, P. and Karotas, S. (2007). Local high-resolution passive seismic tomography and Kohonen neural networks – application at the Rio-Antirio Strait, Central Greece, Geophysics, (72), 93-106,

Thomas, R.J., Marshall, C.G.A., Watkeys, M.K., Fitch, F.J., and Miller J.A. (1992). K–Ar and $^{40}Ar/^{39}Ar$ dating of the Natal Group, South East Africa: a post-pan-African molasse? Journal of African Earth Science (15), 453–471.

Ulusay, R., Turrell, K. and Ider, M.H. (1994). Prediction of engineering properties of a selected litharenite sandstone from its petrographic characteristics using correlation and multi-variate statistical techniques. Engineering Geology investigation of rock strength measures, (37), 135–157.
Vesanto, J. (1999). SOM-based data visualization methods. Intelligent Data Analysis, 3(2), 111-126.
Vesanto, J. and Alhoniemi, E. (2000). Clustering of the self-organizing map. IEEE Transactions on Neural Networks, 11(3), 586-600.